Available online at www.ijpcr.com
International Journal of Pharmaceutical and Clinical Research 2016; 8(12): 1616-1624

ISSN- 0975 1556

Research Article

An Efficient Encapsulation of Thymoquinone Using Solid Lipid Nanoparticle for Brain Targeted Drug Delivery: Physicochemical Characterization, Pharmacokinetics and Bio-Distribution Studies

Surekha R, Sumathi T*

Department of Medical Biochemistry, Dr. ALM Post Graduate Institute of Basic Medical Sciences, University of Madras, Taramani Campus, Chennai – 600 113, Tamil Nadu, India.

Available Online: 25th December, 2016

ABSTRACT

The present study was framed to determine the physicochemical characteristics, stability, *in-vivo* plasma pharmacokinetics and bio-distribution analysis of thymoquinone encapsulated solid lipid nanoparticle (TQ-SLNs) for the brain targeted drug delivery. Fourier transform infrared spectroscopy (FTIR) of TQ-SLNs revealed a possible chemical interaction between the drug and the lipid molecules by showing a shift in the absorption peak of C-H in-plane bend and "oop" band C-H bend stretch of thymoquinone in the lipid core. The thermal behavior of TQ-SLNs revealed a melting enthalpy value of ΔH=131.7 J/g and attained peak at 69.5°C that found to have a greater stability and reduced lipid crystal matrices verifies efficient drug incorporation. Further, the stability analysis of TQ-SLNs showed a stable encapsulation enhancement effect for 6 months. In-addition, the *in-vivo* pharmacokinetic study showed nearly a 5-fold increase in the bioavailability of TQ-SLNs after orally administered to the animals. Further, the drug distribution analysis of TQ-SLNs was found to accumulate more in the brain than other organs, hence suitable for the brain targeted drug delivery.

Keywords: Solid lipid nanoparticles, Thymoquinone, Brain delivery, Pharmacokinetics, Bio-distribution study.

INTRODUCTION

Central nervous system (CNS) is the complex system in the body consisting of the brain and spinal cord[1]. In recent years, an incidence of CNS pathologies increasing worldwide. However, the complicated physiology of the central nervous system (CNS) have been the main limiting factors that disables to attain the therapeutic effects upon the target regions during the systemic administration. This is because of the presence of blood-brain barrier (BBB) that represents the main obstacle for CNS drug development[2,3]. Several strategies have been developed for the sole purpose of an effective drug deposition to the CNS[4,5,6]. Among others, solid lipid nanoparticles (SLNs) have been considered as a proper carrier to overcome BBB issues[7,8]. Solid lipid nanoparticles (SLNs) are colloidal carrier systems that have been developed to encapsulate, protect and deliver lipophilic functional components, such as bioactive lipids and drugs to the CNS[9,10,11,12,13]. Compared to traditional carriers, the SLN combines the advantages of polymeric nanoparticles and oil/water fat emulsions for drug delivery system, such as good tolerability[10,11], high oral bioavailability[12] and large-scale production by high pressure homogenization[13]. In addition, solid lipid matrices have a sustained drug delivery capacity that have been well established for many years and also the typical lipid core helps in controlled release of drugs in the system. Lots of data showed that, SLNs might prolong the release of drug *in-vitro* for many days[14], which made it potential to achieve long-term treatment by using solid lipid nanoparticles as drug carriers. Further, they are found to consider to be a safe and suitable drug carrier for oral delivery of lipophilic drugs.

Thymoquinone is a highly bioactive compound extracted from the oil of *Nigella sativa* seeds, which was found to exhibit various pharmacological activities such as anti-inflammatory[15], anti-oxidation[16], immunomodulatory[17], anti-diabetic[18], anti-nociceptive[19], nephroprotective[20] and neuroprotective[21,22]. Despite of various therapeutic applications this compound suffers from poor solubility and high hydrophobicity leading to poor bioavailability when administered[23]. This problem was solved by nanoparticulate encapsulating system. Earlier we have formulated the thymoquinone encapsulated solid lipid nanoparticles (TQ-SLNs) and some basic characterizations were determined[24]. The developed formulations showed a spherical shaped structure with the particle size of 172.10 ± 7.41 nm with a polydispersity index of 0.225. Similarly, Zeta potential of TQ-SLNs was found to -45.40 ± 2.68 mV. Further, TQ-SLNs showed an entrapment efficiency of 84.49 ± 3.36% with a total drug concentration of 62.35 ± 2.94% in a lipid core. An in-vitro drug release kinetics data revealed a maximum of 86.15 ± 2.76% for TQ-SLNs while 45.52 ± 3.97% for TQ-S in 72 hr, which suggests an initial burst release followed by a controlled release of drug from the TQ-SLNs formulations. Then, the state of formulation was characterized by Powder X-ray diffractometer and it exhibited reduced crystallinity of the entrapped drug whereas TQ alone showed an intense sharp peak and blank

Author for Correspondence: drsumathi.bioscience@gmail.com

SLNs showed diffused peaks. The *in-vitro* cytotoxicity analysis (MTT assay) of developed TQ-SLNs on vero cell culture showed a concentration dependent increase in cytotoxic activity with IC_{50} value of 35.5 ± 10.5 µg/ml. Henceforth, in this study the further characterization of TQ-SLNs using infra-red spectrum, differential scanning calorimetry (DSC), stability analysis, *in-vivo* pharmacokinetics and bio-distribution parameters were conducted to resolve the targeted drug delivery system for the neurological complications.

MATERIALS AND METHODS

Chemicals and Reagents

Thymoquinone was obtained from Sigma Aldrich. Stearic acid, Lecithin and Sodium taurocholate were purchased from Hi-Media chemicals. All the other chemicals used in the present study were of analytical grade and purchased from Merck (India) and Sisco Research Laboratories Pvt. Ltd.

Preparation of Solid lipid nanoparticle encapsulated Thymoquinone (TQ-SLNs)

Stearic acid at a mole fraction of 0.710 was allowed to melt at ~75 °C, simultaneously distilled water was boiled at ~75 °C in a separate beaker. Typically, lecithin, taurocholate and thymoquinone at a mole fraction of 0.210, 0.069 and 0.011 respectively, were added to boiling water on a magnetic stirrer and maintained at ~75 °C. The water–surfactant solution was then added to the melted lipid and again allowed to equilibrate at ~75 °C. The mixture was then homogenized at 24,000 rpm for 150 s to form the emulsion. The obtained hot microemulsion was transferred into an ice cold water (~2 °C), at a ratio of 1:20 (warm microemulsion/cold water) under constant stirring resulting in the formation of solidified lipid nanoparticles. The final product was centrifuged at 20,000×g for 15 min, and nanoparticle pellet was resuspended in distilled water. The preparation was stored at 4 °C for further analysis[25].

Formulation characterization

The nanoparticles obtained were characterized in various parameters described below.

Fourier-transform infrared (FTIR) spectroscopic study

FTIR spectroscopy measurements were carried out to recognize the bio-groups that bound distinctively. The spectrum was recorded for TQ-SLNs, thymoquinone (TQ), SLNs and stearic acid using Spectrum BX infrared spectrophotometer[26]. Samples were prepared in KBr disk (2 mg sample in 200 mg KBr) with a hydrostatic press at a force of 40 psi for 4 min. The scanning range employed was 400–4000 cm^{-1} at a resolution of 4 cm^{-1}.

Differential Scanning Calorimetry (DSC) analysis

Thermograms were recorded with DSC. DSC analysis was performed in order to investigate the melting and recrystallization behavior of TQ-SLNs, thymoquinone (TQ), SLNs and stearic acid. For DSC measurement, 10 mg of samples was put in an open aluminium pan, and then heated at the scanning rate of 10°C/min between 0 and 400°C temperature range under a dry nitrogen atmosphere. Empty aluminum pans were used as standard reference material to calibrate the temperature and energy scale of the DSC apparatus, the entire thermal behavior was studied under a nitrogen purge[27].

Stability studies

TQ-SLNs dispersion was stored at refrigerated temperature (2-8°C) for 6 months under a sealed condition. The average particle size, in-vitro drug release property and physical characteristics were determined periodically after 1, 3 and 6 months[28].

In-vivo pharmacokinetic studies

Male Albino rats weighing 250-300 g were obtained from the Central Animal House, Dr. ALMPGIBMS, University of Madras, Tamil Nadu, India. Rats were housed separately in polypropylene cages and fed a standard pellet diet, kept under hygienic conditions. Rats were kept on a 12 h light and dark cycles with free access to water. All experiments and protocols described in the present study were approved by the Institutional Animal Ethics Committee (IAEC) of Dr. ALMPGIBMS, University of Madras. The in-vivo pharmacokinetic studies were carried out with 12 male Wistar rats divided randomly into 2 groups with 6 animals each. The first group was orally administered a single dose of TQ-SLNs (20 mg/kg). To another group, TQ suspension (20 mg/kg) (TQ dispersed in 4% sodium carboxymethycellulose) (CMC-Na) was administered to obtain a contrast pharmacokinetic behavior with a conventional formulation. 1mL of blood was withdrawn from the retro-orbital plexus under light ether anesthesia at specified time intervals (pre-dose, 0.5, 1, 2, 4, 6, 8, 10, 12, 18, 24 h), into heparinized tubes and immediately centrifuged at 3000 rpm for 15mins. After centrifugation, the plasma obtained was analyzed spectrophotometrically for the concentration of thymoquinone[29].

Biodistribution analysis

Healthy male Wistar rats were randomly divided into 2 groups of 11 animals each. For each group, a single dose of the formulation TQ-SLNs and TQ suspension was administered. After various time intervals (pre-dose, 0.5, 1, 2, 4, 6, 8, 10, 12, 18, 24 h), organs viz. brain, heart, lungs, liver, spleen and kidneys were immediately removed from each group and subjected to homogenization by adding 1mL ice-cold KCl solution per 0.5 g tissue. The supernatant acquired was analyzed spectrophotometrically for thymoquinone concentration[29].

Statistical analysis

All experiments were repeated three times and all measurements were replicated three to five times. Means ± standard deviations were calculated using Microsoft Excel. Statistical significance for the pharmacokinetic analysis was assessed using a one-way analysis of variance (ANOVA) followed by Tukey's *t* test. A $P<0.05$ value was considered statistically significant.

RESULTS AND DISCUSSION

Observation on FT-IR spectrum

The drug lipid interaction was studied by FT-IR spectroscopy and depicted in Fig.1. The IR spectrum of stearic acid (Fig. 1a) revealed the absorption bands at 2918 cm^{-1}, 2850 cm^{-1} (C-H stretch), 1700 cm^{-1} (C=O stretch), 1432 cm^{-1}, 941 cm^{-1} (O-H bend) and 1297 cm^{-1} (C-O

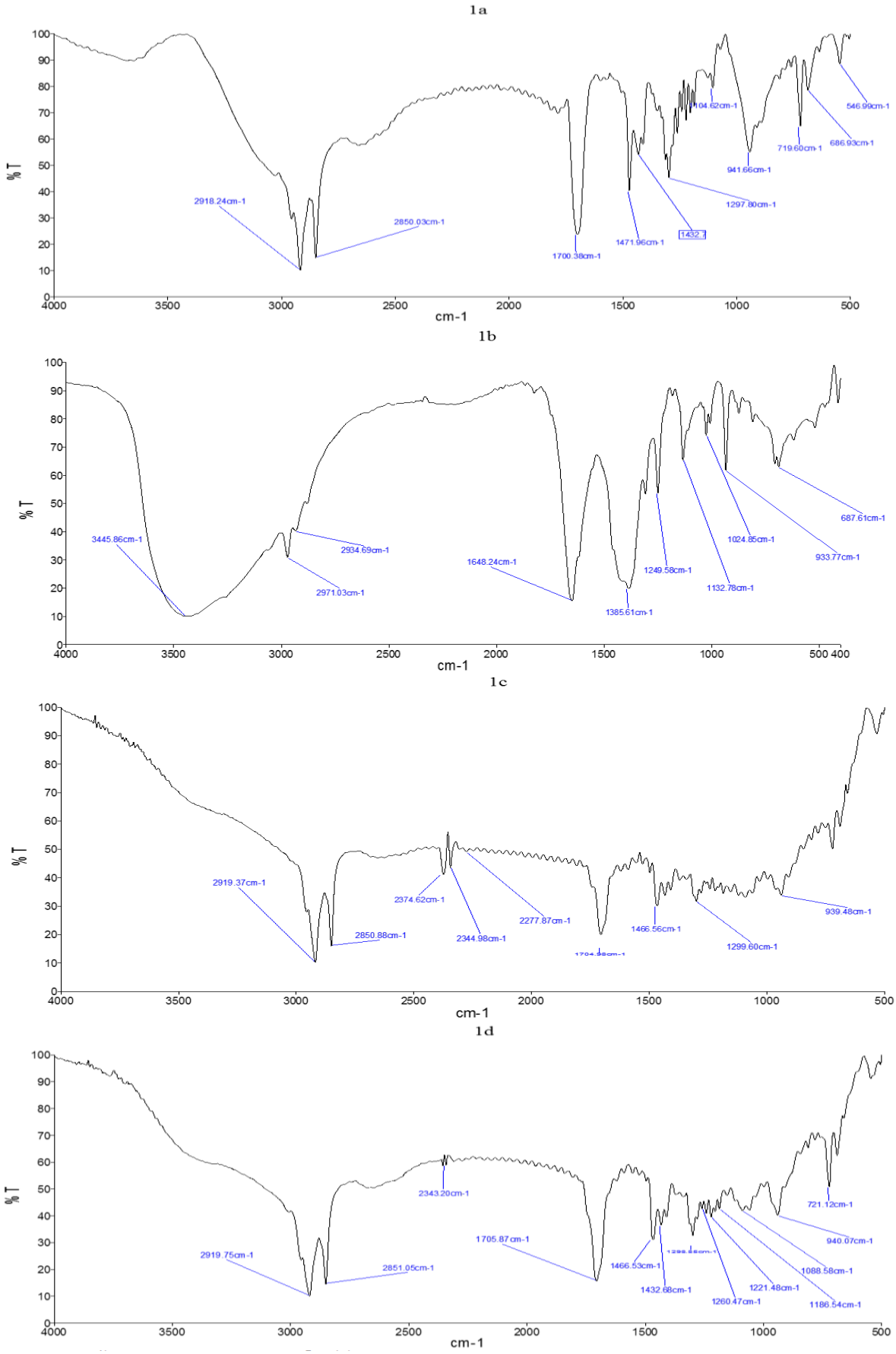

Figure 1: (a) FTIR spectrum of Stearic acid, (b) Thymoquinone drug, (c) B-SLNs and (d) TQ-SLNs.

stretch) (Fig. 1a). For the pure drug (Fig. 1b), IR absorption peaks were recorded at 3445 cm^{-1} (O-H stretch), 2971 cm^{-1}, 2934 cm^{-1} (C-H stretch), 1648 cm^{-1} (C=O stretch), 1385 cm^{-1} (C-H methyl rock), 1249 cm^{-1}, 1132 cm^{-1}, 1024 cm^{-1} (C-H in-plane bend) and 687 cm^{-1} ("oop" band C-H bend). The IR spectrum of blank-SLNs (B-SLNs) (Fig. 1c) revealed the characteristic peaks of stearic acid at 2919 cm^{-1}, 2850 cm^{-1} (C-H stretch), 1704 cm^{-1} (C=O stretch), 1466 cm^{-1} (C-C stretch in-ring) and 1299 cm^{-1} (C-O stretch). Further, the IR spectrum of TQ-SLNs (Fig. 1d) depicted a characteristic absorption peak of stearic acid and thymoquinone which ensures the interaction of the drug to the lipid carrier. However, the intensity of the drug peaks in TQ-SLNs especially C-H in-plane bending were shifted to 1298 cm^{-1}, 1221 cm^{-1}, 1088 cm^{-1}. Also the "oop" band C-H bend peak of thymoquione in the IR spectrum of TQ-SLNs were shifted to 721 cm^{-1}. A shift in the C-H in-plane bend and "oop" band C-H bend indicating the participation of these groups during the encapsulation process of the drug and the lipid molecules. Hence, they signify an extent of interaction which is proportional to the magnitude of the shifts in the stretching frequencies[30].

Thermal analysis of nanoformulation and its constituents using DSC

DSC is an effective method to study the crystallinity of the drug in the compounds or in the carriers by determining at varying temperature and energy. In this study, the DSC curves of stearic acid, blank SLNs (B-SLNs), thymoquinone (TQ), SLN encapsulated thymoquinone (TQ-SLNs) were analyzed. The DSC curves of stearic acid (Fig. 2a) and TQ (Fig. 2b) showed a sharp endothermic peak at 73.6°C and 50.7°C respectively. The melting enthalpy of stearic acid and TQ were found to be 215.8 J/g and 133.3 J/g respectively. Further the melting thermogram of TQ-SLNs (Fig. 2d) showed a sharp peak at 69.5°C with an enthalpy of 131.7 J/g. However, the solubility of a drug in lipid and the presence of lipid imperfections (a space available for the incorporation of drug into the lipid crystal lattice) are important considerations monitoring drug loading. Here, the result of TQ-SLNs proves a decrease in enthalpy change that correlates the loss of crystalline nature or the space availability for the better accommodation of the drug molecule within the lipid crystal lattice. The decrease in crystallinity however, should be maintained during the SLN preparation, thus the enthalpy change and an endothermic peak of B-SLNs was determined, which showed an absorption peak at 68.4°C and enthalpy change at 114.1 J/g (Fig. 2c). This decrease in crystallinity exerts a direct influence on the drug entrapment efficiency and the loading capacity in the lipid core. Thus the reduced crystallinity enables the lipid core (SLNs) to encapsulate the drug efficiently when thymoquinone is added. But an enthalpy range of TQ-SLNs was little higher than B-SLNs that may be due to an encapsulation of the drug thymoquinone in the lipid matrix. Further the change in the melting temperature of TQ-SLNs signifies the derangement in the crystal lattice during the incorporation of TQ to the lipid core and preventing the expulsion of the drug from the SLNs, once they are formulated as a nanoparticles.

Stability analysis

The stability study of TQ-SLNs for the period of 0^{th}, 3^{rd} and 6^{th} month were carried out and depicted in Table 1. The refrigerated TQ-SLNs samples has a maximum particle size of 181.4±6.59 nm and the zeta potential of -35.98±2.17 at 6^{th} month. Further, the stored TQ-SLNs also observed to be opalescent during the period of 6 months and the pH was found to be 7.00±0.07. Also the stored sample was observed for the encapsulation efficiency after 0^{th}, 3^{rd} and 6^{th} month, which were observed to be no significant changes in the encapsulation state of the drug during the period of 6 months storage. The in-vitro drug release data of 0^{th}, 3^{rd} and 6^{th} month samples revealed the maximum of 82.57% of drug released from the stored TQ-SLNs formulations at a period of 72 hr. However, the TQ suspension during the storage of 6 months turned into turbid with a pH of 8.2±0.04. Moreover the percentage of drug encapsulation and in-vitro drug release property were reduced during the storage period. These results indicated that the TQ-SLN was found to have stable physical and chemical configuration and retain their pharmaceutical properties at a storage condition over a period of 6 months.

Plasma pharmacokinetic profile

The pharmacokinetic parameters were applied on plasma concentration–time profiles of TQ-S and TQ-SLNs (Fig. 3), which showed nearly 5 fold increase in the bioavailability of TQ-SLNs ($AUC_{0\rightarrow\infty}$ 2588.992 ± 112.361 µg/ml/h) than TQ–S ($AUC_{0\rightarrow\infty}$ 489.841 ± 27.752 µg/ml/h) after oral administration to the animals and the significant difference is $P<0.05$. Further, the maximum concentration of drug present in the plasma (C_{max} profile), elimination rate constant (K_e), volume of distribution (V_d), total clearance (CL) and plasma half-life ($t_{1/2}$) of TQ-SLNs and TQ-S were listed in Table 2. After the administration of TQ-SLNs and TQ-S to the animals the concentration of drug present in the plasma of TQ-SLNs was found to be increased than TQ-S. Further, the values for K_e, V_d and CL were found to be reduced upon TQ-SLNs administration than TQ-S administration. The rate of clearance and the volume of distribution in an animals were lowered with an increased elimination constant of the drug in SLNs encapsulated state. In contrast, the retention period of the drug (half-life of TQ-SLNs) was found to be increased in the plasma of TQ-SLNs administered animals than TQ-S administered animal plasma, which confirms the formulation to circulate for longer period in the plasma and ensures controlled drug release. However, some of the larger particles of the TQ-SLNs were quickly broken down by the lipases leading to enhanced release of drug in the GIT. The rest of the particles showed characteristic controlled release behavior[31] rather than TQ-S.

Pharmacokinetic parameters are represented as mean ± SD (n=6). $^{a}P<0.05$ shows statistically significant compared to TQ-S administered group. $AUC_{0-\infty}$ – Area under the concentration-time curve from zero to infinity; C_{max} – Maximum concentration achieved in the blood; T_{max} – Time needed to reach maximum concentration; Ke –

2a

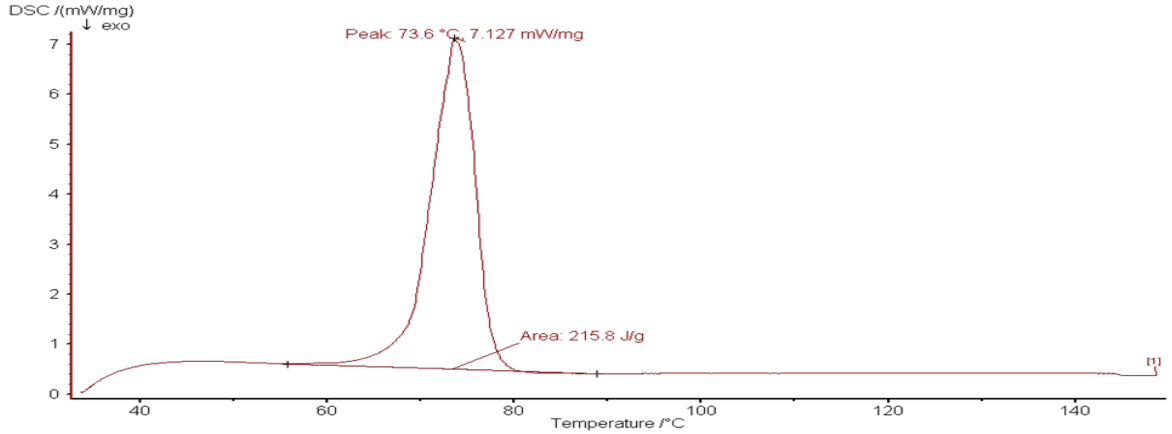

2b

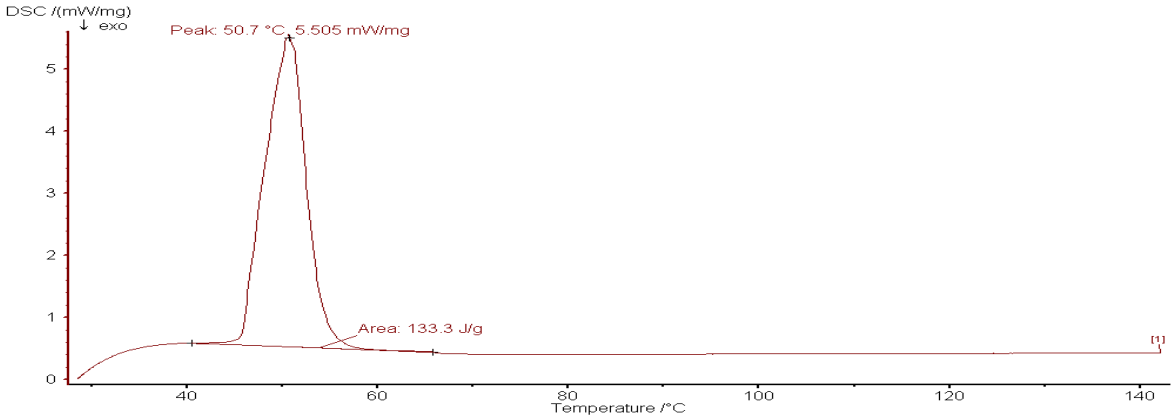

2c

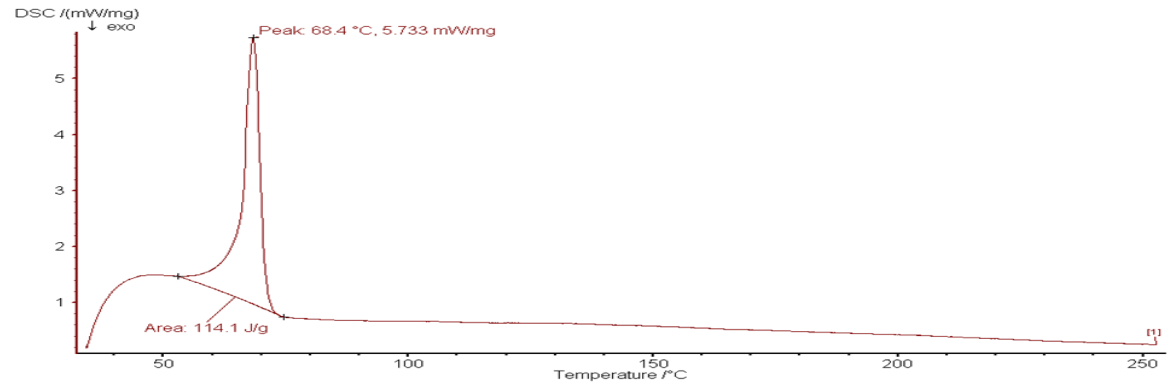

2d

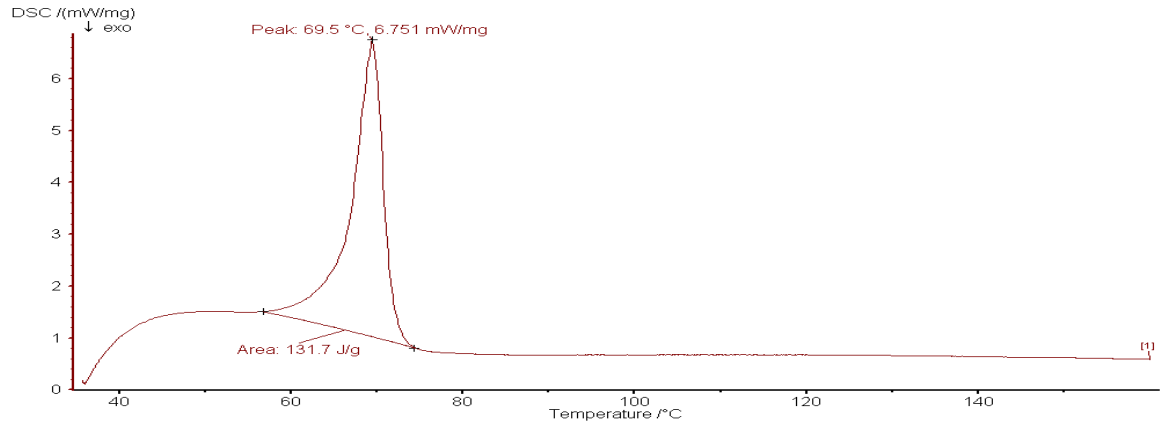

Figure 2: (a) DSC thermogram of Stearic acid, (b) Thymoquinone drug,(c) B-SLNs and (d) TQ-SLNs.

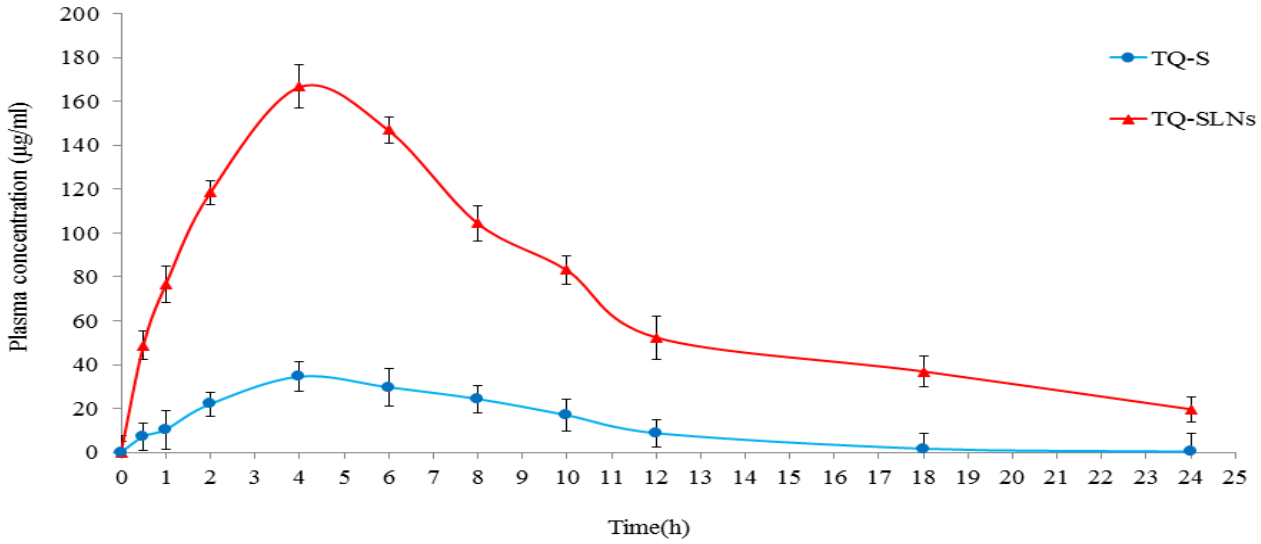

Figure 3: Plasma pharmacokinetic profile of TQ-SLNs and TQ-S at various time periods.

Table 1: Examination of refrigerated samples (TQ-SLNs and TQ-S) for its physicochemical characteristics after a regular intervals of time.

Stability tests	TQ-SLNs			TQ-S		
Period (month)	0	3	6	0	3	6
Sample clarity	Opalescent	Opalescent	Opalescent	Clear	Turbid	Turbid
Sediment formation	No	No	No	No	Yes	Yes
pH ± SD	7.00±0.05	7.03±0.02	7.00±0.07	7.05±0.06	7.54±0.13	8.2±0.04
Particle size ± SE(nm)	172.1±7.41	178.2±6.73	181.4±6.59	1569±7.56	1684±13.46	1820±15.68
PDI ± SE	0.225±0.05	0.274±0.06	0.312±0.03	0.753±0.12	0.813±0.26	0.896±0.33
Maximum drug release in 72h ± SE (%)	86.15±2.76	84.98±3.51	82.57±2.68	45.52±3.97	36.87±4.21	32.42±3.19

Stability tests are represented as mean ± SD/SE (n=3).

Table 2: Pharmacokinetics parameters of thymoquinone after oral administration of TQ-SLNs and TQ-S to the animals.

Pharmacokinetic Profiles	TQ-SLNs	TQ-S
$AUC_{0-\infty}$ (µg/ml/h)	2588.992 ± 112.361[a]	467.398 ± 27.752
C_{max} (µg/ml)	166.649 ± 22.616[a]	34.507 ± 4.201
T_{max} (h)	4	4
Ke (h^{-1})	0.104 ± 0.02	0.271 ± 0.04
Vd (L)	0.074 ± 0.08	0.147 ± 0.12
$t_{1/2}$ (h)	6.663 ± 0.21[a]	2.557 ± 0.08
CL_{total} (Lh^{-1})	0.007 ± 0.002	0.040 ± 0.011

Elimination rate constant; Vd – Volume of distribution; $t_{1/2}$ – Elimination half-life; CL_{total} – Total clearance.

Improved brain drug delivery

The drug deposition in various organs post oral administration was verified over time for TQ-SLNs and TQ-S (Fig. 4a-f). The major concentration of TQs was accumulated significantly ($P<0.05$) in brain with higher area under the concentration-time curve from zero to infinity ($AUC_{0\rightarrow\infty}$) when it was encapsulated with SLNs than TQ suspension. Figure. 4 depicts the comparative graphical representation of the bio-distribution analysis of TQ-SLNs and TQ-S in different organs. The drug distribution ranges in various organs as follows: Brain ($AUC_{0\rightarrow\infty}$ 66.921 ± 2.505 µg/g/h) > Liver ($AUC_{0\rightarrow\infty}$ 21.704 ± 2.395 µg/g/h) > Kidney ($AUC_{0\rightarrow\infty}$ 17.441 ± 1.946 µg/g/h) > Spleen ($AUC_{0\rightarrow\infty}$ 13.461 ± 2.548 µg/g/h) > Heart ($AUC_{0\rightarrow\infty}$ 11.4 ± 3.641 µg/g/h) > Lung ($AUC_{0\rightarrow\infty}$ 1.118 ± 3.725 µg/g/h). Tissue bio-distribution proved that the TQ-SLN formulations were found to accumulate more in the brain and less in the reticulo-endothelial tissues due to its size and composition. The decreased uptake of TQ-SLNs by the liver and spleen enhances its bioavailability to non-RES organs, especially the brain[31]. Similarly, influx of drug through endocytosis or transcytosis and efflux of the drug from the brain to the plasma were controlled by surfactants and co-surfactants of the formulations thereby accumulating major concentration of the drug to the

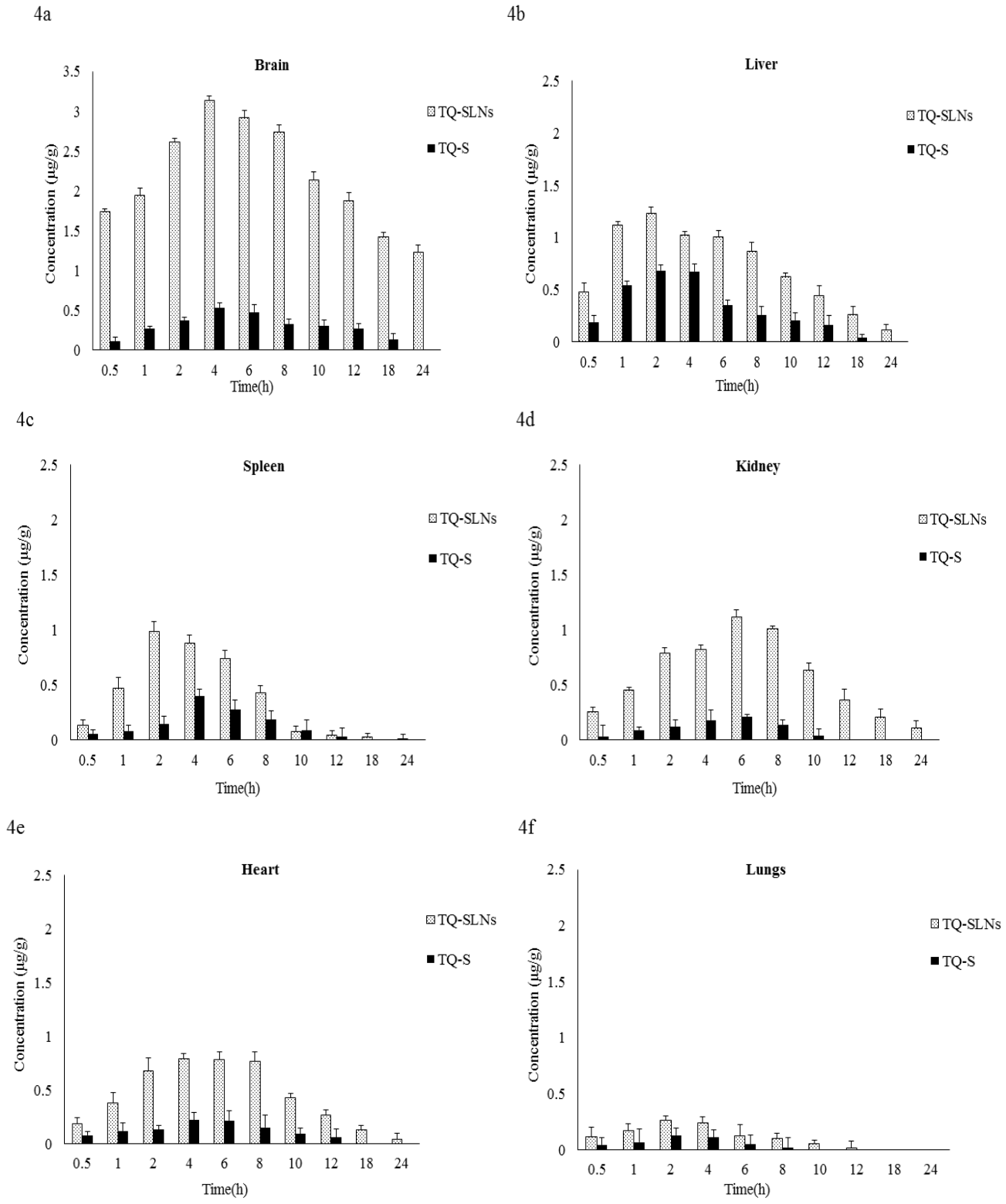

Figure 4 (a-f): Tissue distributions of thymoquinone after an oral administration of TQ-SLNs and TQ-S at various time periods.

brain[32]. Conversely, the suspension TQ due to its metabolic site it was found to accumulate more in the liver rather than reaching the target organ brain. Also the $AUC_{0\rightarrow\infty}$ level of TQ-S was found to be lower in all the organs when compared to TQ-SLNs, which infers that the formulated solid lipid nanoparticle encapsulated thymoquinone (TQ-SLNs) effectively targets the drug towards the brain.

CONCLUSION

The present study highlights the physio-chemical characteristics, pharmacokinetic profile and tissue

distribution properties of the formulated thymoquinone loaded solid lipid nanoparticles (TQ-SLNs). The observation on FTIR and DSC studies clearly demonstrate that the drug has a stronger interaction with the lipid matrix and the thermal behavior implies reduction in the crystallinity signifies efficient encapsulation. TQ-SLNs formulation was also found to be stable for 6 months with an insignificant change in the stability parameters. Further the pharmacokinetics and bio-distribution data revealed that the formulation efficiently targets the brain and delivers the drug in a controlled manner to the target organ. Furthermore TQ-SLNs was found to have increased bio-availability and plasma half-life than TQ suspension. Thus, the TQ-SLNs formulation was considered as a well-suitable preparation to treat the age related brain diseases in a better way using an innovative tool.

ACKNOWLEDGEMENT

The first author is grateful to UGC for the financial support in the form of JRF – UGC – BSR Fellowship. And also, the authors thank **"**Sophisticated analytical instrument facility (SAIF), Indian Institute of Technology-Madras, India" for providing Differential scanning calorimetry facility to perform the thermal behavior of nanoformulation.

REFERENCES

1. Pardridge WM. Why is the global CNS pharmaceutical market so under-penetrated? Drug Discov Today. 2002; 7(1):5–7.
2. Lawrence RN, Pardridge W. Discusses the lack of BBB research. Drug Discov Today. 2002; 7(4):223–226.
3. Begley DJ. Delivery of therapeutic agents to the central nervous system: the problems and the possibilities. Pharmacol Ther. 2004; 104(1):29–45.
4. Johanson CE, Duncan JA, Stopa EG, Baird A. Enhanced prospects for drug delivery and brain targeting by the choroid plexus-CSF route. Pharm Res. 2005; 22(7):1011–1037.
5. Gaillard PJ, Visser CC, De Boer AG. Targeted delivery across the blood-brain barrier. Expert Opin Drug Deliv. 2005; 2(2):299–309.
6. Badruddoja MA, Black KL. Improving the delivery of therapeutic agents to CNS neoplasms: a clinical review. Front Biosci. 2006; 11:1466–1478.
7. Garcia-Garcia E, Andrieux K, Gil S, Couvreur P. Colloidal carriers and blood-brain barrier (BBB) translocation: a way to deliver drugs to the brain? Int J Pharm. 2005; 298(2):274–292.
8. Muller RH, Keck CM. Drug delivery to the brain-realization by novel drug carriers. J Nanosci Nanotechnol. 2004; 4(5):471–483.
9. Muller RH, Mader K, Gohla S. Solid lipid nanoparticles (SLN) for controlled drug delivery - A review of the state of the art. Eur J Pharm Biopharm. 2000; 50(1):161–177.
10. Muller RH, Maaben S, Weyhers H, Specht F, Lucks JS. Cytotoxicity of magnetide-loaded polylactide, polylactide/glycolide particles and solid lipid nanoparticles. Int J Pharm. 1996; 138(1):85–94.
11. Maaben S, Schwarz C, Mehnert W, Lucks JS, Yunis-Specht F, Muller BW, Muller RH. Comparison of cytotoxicity between polyester nanoparticles and solid lipid nanoparticles. Proc Int Symp Control Release Bioact Mater. 1993; 20:490–493.
12. Yang SC, Zhu JB, Lu Y, Liang BW, Yang CZ. Body distribution of camptothecin solid lipid nanoparticles after oral administration. Pharm Res. 1999; 16(5):751–757.
13. Muller RH, Lucks JS. Arzneistoffträger aus festen Lipidteilchen, Feste Lipidnanosphären (SLN). European Patent No.0605497, 1996.
14. Muller RH, Mehnert W, Lucks JS, Schwarz C, Zur Muhlen A, Meyhers H, Freitas C, Ruhl D. Solid-lipid nanoparticles (SLN): an alternative colloidal carrier system for controlled drug delivery. Eur J Pharm Biopharm. 1995; 41(1):62–69.
15. Ghannadi A, Hajhashemi V, Jafarabadi H. An investigation of the analgesic and anti-inflammatory effects of *Nigella sativa* seed polyphenols. J Med Food. 2005; 8(4):488–493.
16. Kanter M, Coskun O, Uysal H. The anti-oxidative and anti-histaminic effect of *Nigella sativa* and its major constituent, thymoquinone on ethanol-induced gastric mucosal damage. Arch Toxicol. 2006; 80(4):217–224.
17. El-Kadi A, Kandil O. The black seed (*Nigella sativa*) and immunity: its effect on human T cell subset. Fed Proc. 1987; 46(4):1222.
18. Abdelmeguid NE, Fakhoury R, Kamal SM, Al Wafai RJ. Effects of *Nigella sativa* and thymoquinone on biochemical and subcellular changes in pancreatic β-cells of streptozotocin-induced diabetic rats. J Diabetes. 2010; 2(4):256–266.
19. Ansari MA, Ahmad SJ, Khanum R, Akhtar M. Pharmacological investigation of protective effects of *Nigella sativa* oil in experimental diabetic neuropathy in rats. Indian J Pharm Educ Res. 2009; 43(2):166–176.
20. Badary OA, Nagi MN, Al-Shabanah OA, Al-Sawaf HA, Al-Sohaibani MO, Al-Bekairi AM. Thymoquinone ameliorates the nephrotoxicity induced by cisplatin in rodents and potentiates its antitumor activity. Can J Physiol Pharmacol. 1997; 75(12):1356-1361.
21. Alhebshi AH, Gotoh M, Suzuki I. Thymoquinone protects cultured rat primary neurons against amyloid β-induced neurotoxicity. Biochem Bioph Res Co. 2013; 433(4):362–367.
22. Celik F, Gocmez C, Karaman H, Kamasak K, Kaplan I, Akil E, Tufek A, Guzel A, Uzar E. Therapeutic Effects of Thymoquinone in a Model of Neuropathic Pain. Curr Ther Res Clin Exp. 2014; 76(2):11–16.
23. Odeh F, Al-Jaber H, Khater D. Application of nanotechnology in drug delivery. Intech, Europe, 2014.
24. Surekha R, Aishwarya V, Sumathi T. Thymoquinone loaded solid lipid nanoparticle: Formulation, characterization and in-vitro cell viability assay. Int J Pharm Bio Sci. 2015; 6(1):449-464.
25. Frautschy SA, Cole GM. Bioavailable curcuminoid formulations for treating Alzheimer's disease and other

age-related disorders, United states, US:2009/0324703 A1, 2009.
26. Madan J, Pandey RS, Jain V, Katare OP, Chandra R, Katyal A. Poly (ethylene)-glycol conjugated solid lipid nanoparticles of noscapine improve biological half-life, brain delivery and efficacy in glioblastoma cells. Nanomedicine: Nanotechnology, Biology, and Medicine 2013; 9(4):492–503.
27. Dodiya SS, Chavhan SS, Sawant KK, Korde AG. Solid lipid nanoparticles and nanosuspension formulation of Saquinavir: preparation, characterization, pharmacokinetics and biodistribution studies. J Microencapsul. 2011; 28(6):515–527.
28. Venishetty VK, Samala R, Komuravelli R, Kuncha M, Sistla R, Diwan PV. β-Hydroxybutyric acid grafted solid lipid nanoparticles: A novel strategy to improve drug delivery to brain. Nanomedicine: Nanotechnology, Biology, and Medicine 2013; 9(3):388–397.
29. Geetha Rani V, Sugumaran M, Appaji Rao N, Vaidyanathan CS. A new colorimetric methods for the estimation of quinones, Colorimetric estimation of quinones. 1978; 43-50.
30. Rohit B, Indu Pal K. A Method to Prepare Solid Lipid Nanoparticles with Improved Entrapment Efficiency of Hydrophilic Drugs. Curr Nanosci. 2013; 9(2), 1-10.
31. Singh A, Ahmad I, Akhter S, Jain GK, Iqbal Z, Talegaonkar S, Ahmad FJ. Nanocarrier based formulation of Thymoquinone improves oral delivery: Stability assessment, in vitro and in vivo studies. Colloid Surface B. 2013; 102(1):822–832.
32. Vankateswarlu V, Manjunath K. Preparation, characterization and in-vitro release kinetics of clozapine solid lipid nanoparticles. J Control Rel. 2004; 95(3):627-638.